Oxygen adsorption on W(001) studied by low energy (e,2e) spectroscopy

S. Samarin, J. Berakdar, R. Herrmann, H. Schwabe,
O. Artamonov* and J. Kirschner

Max-Planck-Institut für Mikrostrukturphysik, Weinberg 2, 06120 Halle, Germany
** Research Institute of Physics, St. Petersburg University, Uljanovskaja 1, Petrodvoretz, St. Petersburg 198904, Russia*

Abstract.

We applied the low energy (e,2e) spectroscopy in reflection-mode scattering geometry for studying ordered oxygen adsorption on W(001). Primary electrons with the energy of 36 eV were used to excite the correlated electron pairs from a p(2x1) adsorbed oxygen layer. The (e,2e) spectra of clean and oxygen covered W(001) surface were analyzed. It was found that the adsorption of 1 ML of oxygen on W(001) leads to the appearance of an additional structure in the energy distribution of correlated pairs. This structure corresponds to the excitation of electrons from the energy level located at $6.7 \pm 0.5\,eV$ below the Fermi level. This result is consistent with the UPS study of the oxygen adsorption on W(001) [1] where the adsorbate photoemission peak was observed at 6.5 eV below Fermi level. A theoretical analysis of the emission process is developed and used to explain the main structures in the observed electron pair spectra.

1. INTRODUCTION

Adsorption of oxygen on the (001) surface of tungsten has been investigated by various techniques, e. g., by photoelectron spectroscopy, LEED, Auger spectroscopy, EELS... [1,2,3,4,5]. It was found that the oxygen molecules dissociate into their constituate atoms upon adsorption on tungsten. At small coverage the oxygen atoms are well ordered on the W(001) surface and the oxygen layer admits a variety of structures depending on the temperature of the sample during adsorption, the temperature treatment after adsorption and on the amount of oxygen atoms [1]. The electronic structure of the substrate surface and the free oxygen atom are considerably modified by the adsorption process. This has been seen evidently in the spectra of photoelectron emitted from the adsorbate system: some of the maxima in the spectra of the clean substrate disappear after adsorption while some new maxima appear for the adsrobate system [1].

The above mentioned methods supply the detailed information about geometrical structure of the oxygen adsorbed layer and energy positions of the adsorbate electronic states. On the other hand the (e,2e) spectroscopy under favorable conditions yields, in addition to the electronic structure information [6-9], a direct insight into the inter-electronic correlation of the excited electron pair and their coupling to other degree of freedom of the system [14]. In a previous work [14] we investigated the dynamics of electron pair emission from delocalized electronic states of Cu(001) and Fe(011). In the present work the electronic

states of the adsorbed oxygen layer are localized and hence the emission dynamics is expected to resemble that found for atomic targets. To substantiate this suppostion we developed a theoretical formulation of the pair emission from the adsobed systems. The measured spectra are contrasted against the theoretical predictions and the corresponding situation for free oxygen target.

2. THEORETICAL CONSIDERATIONS

The chemisorption process results in a strong modification of the electronic properties of the surface and the adsorbate atoms. For example, surface states of the substrates are suppressed [13] and the energy levels of the adsorbate are shifted and broadened. Thus an adequate theoretical treatment of this process should account for these modification, at least in the region where they are most pronounced. The electron-pair emission probability from the "adsorbate system" (adsorbate and substrate) is related to

$$\frac{d\sigma(\mathbf{k}_1,\mathbf{k}_2)}{d^3\mathbf{k}_1 d^3\mathbf{k}_2} = \frac{(2\pi)^4}{k_0} \sum_{\alpha,\beta} \int d^3\mathbf{k}_j \rho_{dos}\left(\epsilon(\mathbf{k}_j)\right)\, F(\epsilon(\mathbf{k}_j),T)|\mathcal{T}|^2 \delta(E_f - E_i) \tag{1}$$

where $\mathbf{k}_1$ and $\mathbf{k}_2$ are the wave vectors of the vacuum electrons, $\rho_{dos}(\epsilon(\mathbf{k}_j))$ is the density of states of the bound electron with energy ϵ and wave vector $\mathbf{k}_j$, $\mathbf{k}_0$ is the projectile's incident momentum, E_i (E_f) is the total energy in the initial (final) state and F is the Fermi distribution at temperature T. Eq.(1) sums over final states degeneracy β, and over non-observed initial states α. As clear from Eq.(1), only the on-shell, i. e. the energy-conserving, part of the transition matrix $\mathcal{T}$ is important. This amplitude is, to first order the sum of two amplitudes: T^{sub} and T^{ad}, where T^{sub} and T^{ad} describe the pair emission from the substrate and from the p(2x1) adsorbed oxygen layer, respectively. The amplitude T^{sub} has the form [14]

$$T^{sub} = \delta^{(2)}(\mathbf{K}_{0,\|} - \mathbf{K}^+_{\|})\, \Lambda' + C \sum_{\ell,\mathbf{g}^{sub}_{\|}} \delta^{(2)}[\mathbf{g}^{sub}_{\|} - (\mathbf{K}^+_{\|} - \mathbf{K}_{0,\|})]\, \Lambda. \tag{2}$$

where $\mathbf{K}_0 = \mathbf{k}_0 + \mathbf{k}$ is the initial wave vector of the pair and $\mathbf{K}^+ = \mathbf{k}_1 + \mathbf{k}_2$ is it's final wave vector. $\mathbf{g}^{sub}_{\|}$ is the surface reciprocal substrate-lattice vector and ℓ enumerates the substrate atomic layers. The functions C, Λ, Λ' depend on the dynamical description of the process and can be calculated, e. g., as in Ref.[14]. The first term of Eq.(2) describes the direct transition of the pair into the vacuum level, whereas the second term accounts for the diffraction of the pair from the substrate lattice.

Similarly the transition amplitude for the pair emission from the superlattice is the sum of two amplitudes T^{ee}, the direct pair-ejection amplitude, and T^{core}, the amplitude that describes the pair's diffraction from the superlattice, i. e.

$$T^{ad} = T^{ee} + T^{core}. \tag{3}$$

where $T^{ee} = \langle\Psi|V_{ee}|\mathbf{k}_0,\Phi\rangle$, $T^{core} = \langle\Psi|V_{core}|\mathbf{k}_0,\Phi\rangle$. Here $\langle\Psi|$ is the pair's state propagating outwards into the detectors' states $|\mathbf{k}_1,\mathbf{k}_2\rangle$, $|\Phi\rangle$ is the electronic state of the adsorbate, V_{ee} is the electron-electron interaction and V_{core} is the superlattice scattering potential. In what follows we consider the case of a perfect monolayer ($\theta = 1$). Since the lattice constant of the oxygen superlattice is larger than the extent of the active atomic orbitals we may employ a tight-binding description for the electronic wave function of the oxygen monolayer:

$$\Phi_{\mathbf{k}_{\|}}(\mathbf{r}_2) = N \sum_j \exp(i\mathbf{k}'_{\|}\cdot\mathbf{R}_{\|,j})\varphi(\mathbf{r}_{2,\|} - \mathbf{R}_{j,\|}, \mathbf{r}_{2,z} - d). \tag{4}$$

Here $\varphi(\mathbf{r}_{2,\|} - \mathbf{R}_{j,\|}, \mathbf{r}_{2,z} - d)$ is an atomic orbital localized at the site $(\mathbf{R}_{j,\|}, d)$ where d is the distance between the adsorbed layer and the surface layer (for the present case $d = 1.25$ A°), $\mathbf{k}'_{\|}$ is a two-dimensional Bloch

wave vector and $\mathbf{r}_2$ is the position vector of the bound electron. Following the emission process we assume the superlattice to be neutralized by the substrate on a time scale much faster than the ejection process. In this case the following assumption for the two-electron state is reasonable:

$$|\Psi\rangle = (1 + G_{ee}V_{ee})|\mathbf{k}_1, \mathbf{k}_2\rangle \tag{5}$$

where G_{ee} is the propagator within the pontetial V_{ee}. Under the above assumptions the amplitudes T^{ee} and T^{core} can be written as

$$\begin{aligned} T^{ee} &= N_c\mathcal{N}\sum_j \int d^3\mathbf{r}_1 d^3\mathbf{r}_2 \exp(i\mathbf{q}\cdot\mathbf{r}_1 - i\mathbf{k}_2\cdot\mathbf{r}_2)\bar{\Psi}(\mathbf{r}_1,\mathbf{r}_2)\,V_{ee} \\ &\qquad \exp(i\mathbf{k}'_{\|}\cdot\mathbf{R}_{j,\|})\varphi(\mathbf{r}_{2,\|} - \mathbf{R}_{j,\|}, \mathbf{r}_{2,z} - d) \end{aligned} \tag{6}$$

$$\begin{aligned} T^{core} &= -N_c\sum_{kl}\int d^3\mathbf{r}_1 d^3\mathbf{r}_2 \frac{Z_t}{|\mathbf{r}_{1,\|} - \mathbf{R}_{l,\|}| + |r_{1,z} - dl|}\exp(i\mathbf{q}\cdot\mathbf{r}_1 - i\mathbf{k}_2\cdot\mathbf{r}_2) \\ &\qquad \bar{\Psi}(\mathbf{r}_1,\mathbf{r}_2)\exp(i\mathbf{k}'_{\|}\cdot\mathbf{R}_{k,\|})\varphi(\mathbf{r}_{2,\|} - \mathbf{R}_{j,\|}, \mathbf{r}_{2,z} - d). \end{aligned} \tag{7}$$

Here $\mathcal{N}$ is the number of the oxygen sites, N_c is a normalization constant, Z_t is the core charge, $\bar{\Psi}$ is a (confleunt hypergeometric) function that can be deduced from the solution of Eq.(5), $\mathbf{r}_1$ is the position vector of the incident electron, and $\mathbf{q} = \mathbf{k}_0 - \mathbf{k}_1$ is the momentum transfer vector. The multi-center *hopping integrals* involved in Eq.(7) are quite complicated to calculate. However, as φ is well localized on the scale of the superlattice constant, the main contributions to (7) originate from the *on-site* emission, i.e. for $k = l$. Furthermore, if we assume, as usually done (see e.g. [1]), that the electron-pair current is the incoherent sum of the currents from the substrate and the adsorbate the cross section for the pair emission becomes proportional to $|T^{sub}|^2 + |T^{ad}|^2$ where $|T^{ad}|^2$ is obtained after some algebraic manipulation from Eqs.(3,6,7) to be

$$|T^{ad}|^2 = \sum_{\mathbf{g}^{ad}_{\|}} \delta^{(2)}[\mathbf{g}^{ad}_{\|} - (\mathbf{K}^{+}_{\|} - \mathbf{K}'_{0,\|})]\,|\bar{T}^{ee} + \bar{T}^{core}|^2 \tag{8}$$

where $\mathbf{K}'_{0,\|} = \mathbf{k}_{0,\|} + \mathbf{k}'_{\|}$ and

$$\bar{T}^{ee} = N_c \exp[i(q_z - k_{b,z})d]\int d^3\rho_1 d^3\rho_2 \exp(i\mathbf{q}\cdot\rho_1 - i\mathbf{k}_2\cdot\rho_2)\bar{\Psi}(\rho_1 - \rho_2)\,V_{ee}\varphi(\rho_2) \tag{9}$$

$$\bar{T}^{core} = -N_c \exp[i(q_z - k_{b,z})d]\int d^3\rho_1 d^3\rho_2 \frac{Z_t}{\rho_1}\exp(i\mathbf{q}\cdot\rho_1 - i\mathbf{k}_2\cdot\rho_2)\bar{\Psi}(\rho_1 - \rho_2)\varphi(\rho_2). \tag{10}$$

The transitional factor $\exp[i(q_z - k_{b,z})d]$ is irrelavent for the cross section. From Eqs.(2.8), it is clear that we obtain two types of diffraction:1) diffraction of the pair from the W(001) lattice with the maximum width of the diffraction maxima being given basically by k_F where k_F is the Fermi wave vector of the substrate state, and 2) diffraction from the superlattice with the shape of these diffraction maxima being determined by $|\bar{T}^{ee} + \bar{T}^{core}|^2$, as evident from Eq.(8). The interference between the electron-pair currents from the substrate and the superlattice are described by the term $(T^{ad})^* T^{sub} + T^{ad}(T^{sub})^*$.

3. EXPERIMENT

In order to increase the efficiency of the detection of correlated electron pairs and keeping in mind that we are going to deal with low energy electrons, we combined the coincidence technique with the time-of-flight

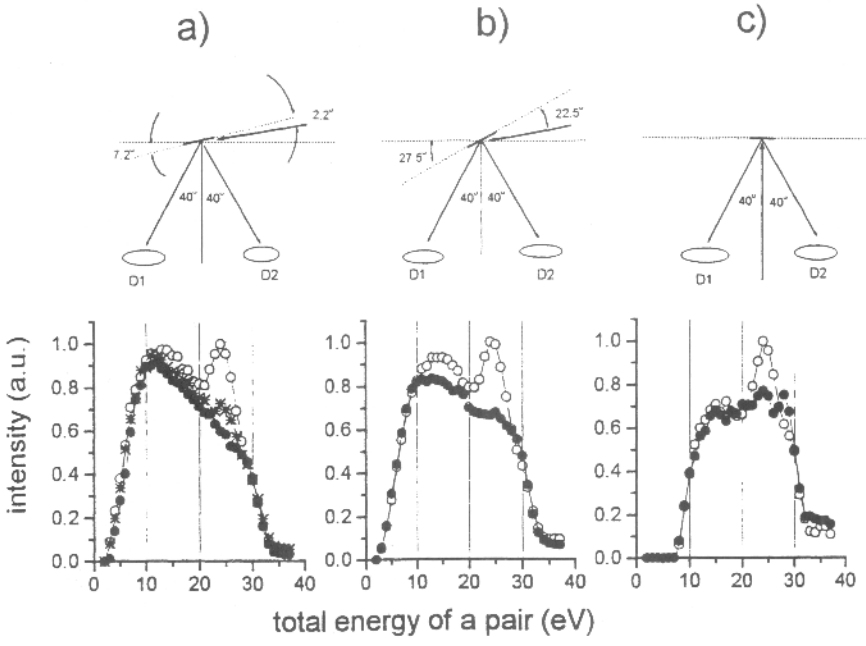

Figure 1: The total energy distributions for clean and oxygen covered W(001). The primary electron energy is 36 eV. Solid circles: clean tungsten, open circles: tungsten + 1 ML of oxygen, stars: tungsten + 0.5 ML of oxygen. The geometries of the experiment are shown in the upper parts of the panels.

technique for measuring the kinetic energy of electrons. The principle of the time-of-flight electron energy measurement is described elsewhere [10,11,12]. The W(100) crystal was mounted on a rotatable holder. The sample cleaning procedure included oxidation of the sample followed by high temperature flashes to remove carbon from the sample surface. The cleanliness of the surface was monitored by Auger electron spectroscopy and LEED. The incident electron current of the order of 10^{-14} A, on average, was pulsed with a width of about 1 ns and a repetition rate of 2.5 10^6 pulses per second in order to measure the time-of-flight spectra. To detect the electrons we used two 75 mm MCP-based position sensitive electron detectors. The detectors and the electron gun were in the same plane containing the sample surface normal. The position sensitive detectors allow us to control the electron beam position on the sample by observing the specular beam as well as the diffracted beams. They also allow us to control the position of the sample and to observe the LEED patterns from the adsorbed layer of oxygen. The base pressure in the vacuum chamber was in the range of 10^{-11} Torr. We performed the oxygen adsorption using as reference the data from [1].

We exposed a clean W(001) surface to oxygen with an exposure of 10 L which corresponds to the coveraged of one monolayer. The sample is then heated up to 1400 C^o. The structure was checked by LEED.

For a given incident electron energy, the measured two-dimensional time-of-flight distributions of correlated electron pairs were converted into the two-dimensional energy distributions of pairs. Each point on this distribution represents a correlated pair of electrons with the energies E_1 and E_2. The analysis

of the energy distribution of correlated pairs consists of calculating the number of pairs within the total energy bands $E_{tot} \pm \Delta E$, where $E_{tot} = E_1 + E_2$. If we take the width of the total energy bands equal to 1 eV, then all events within these bands have the sum of energies of two correlated electrons equal to $E_{tot} \pm 0.5\,eV$. We calculate the number of events within such bands for different E_{tot} and we end up with the distribution of correlated electron pairs as a function of the total energy of the pair. This spectrum we call "total energy distribution". The cut-off of the distribution at the high energy side corresponds to the pair excitation from the highest occupied energy levels (vicinity of the Fermi level). The pairs with lower total energy are excited from deeper energy levels. That means the total energy, E_{tot}, of a pair corresponds to a certain binding energy of the valence electron E_b which is excited by the incident electron with energy E_i, i .e. $E_b = E_i - E_{tot}$.

Further analysis of the energy distribution of correlated pairs is made by calculating the number of events within total energy band $E_{tot} \pm 0.5\,eV$ with a certain combination of energies E_1 and E_2 of both correlated electrons which is represented by the difference $\Delta = (E_1 - E_2) \pm 0.5\,eV$. This distribution of pairs as a function of the difference energy $(E_1 - E_2)$ is called "energy sharing distribution".

4. RESULTS AND DISCUSSION

From the photoemission data Ref.[1] it has been concluded that the electronic state of the oxygen adsorbate is located $6.5\,eV$ below the Fermi level E_F. In the present study, the incident energy E_i has been chosen as $36\,eV$. Thus, due to enhancement in the total density of states of the adsorbate system, we expect (cf. Eq.(1)) an increase in the binding energy spectrum at $6.5\,eV$ below E_F, i. e. at $E_{tot} \approx 36 - 6.5 - W = 25\,eV$ where W is the work function. To clearly see the influence of the adsorbate state we investigate the total energy distributions for clean and oxygen covered W(001) surfaces. The two spectra are normalized by the acquisition time the incident current being constant. As clearly seen in Fig.1, an additional maximum appears in the spectrum for W(001) + oxygen at $E_{tot} \approx 25\,eV$ and gradually increases with increased coverage (see Fig.1a). The energy width of this maximum reflects the energy-broadening of the $2p$ state of atomic oxygen due to coupling to the substrate. This is substantiated by the fact that the position and the width of the maximum at $E_{tot} = 25\,eV$ is virtually not changing for different scattering geometry (cf. Figs.1a,b,c). On the other hand the binding energy spectrum of clean W(001) is very much dependent on the geomtrical arrangemtns of the detectors. This is due to the fact that electron pairs emitted from tungesten are subject to inelastic scattering processes that are sensitive to the scattering geometry.

Figs. 1(a.b,c) do not resolve the energies E_1 and E_2 of the individual electrons and contain thus only intgral information on the emission process.

To get more insight into the emission process we investigate for a given total energy $E_{tot} = 25\,eV$ the energy-sharing distributions of the escaping electrons. This total energy corresponds to electron excitation from the adsorbate state. Such a spectrum has been analysed in details for the electron-pair emission from delocalized electronic states, namely from the conduction band of Cu(001) and Fe(011). Thus, to get some insight into the pair emission from localized states, we focus here on difference of the spectra for clean and covered surface: [W(001) + oxygen] - [W(001)]. This difference should provide clear information on the emission from the adsorbate state. As argued in a previous work [14] and as evident from Eqs.(2,8), the effect of diffraction is most transperant when the spectra are analysed as function of $K_{\parallel}^{+}$. In the present experiment the electron-pair current can be measured as function of the component of $K_{\parallel}^{+}$ in the plane of

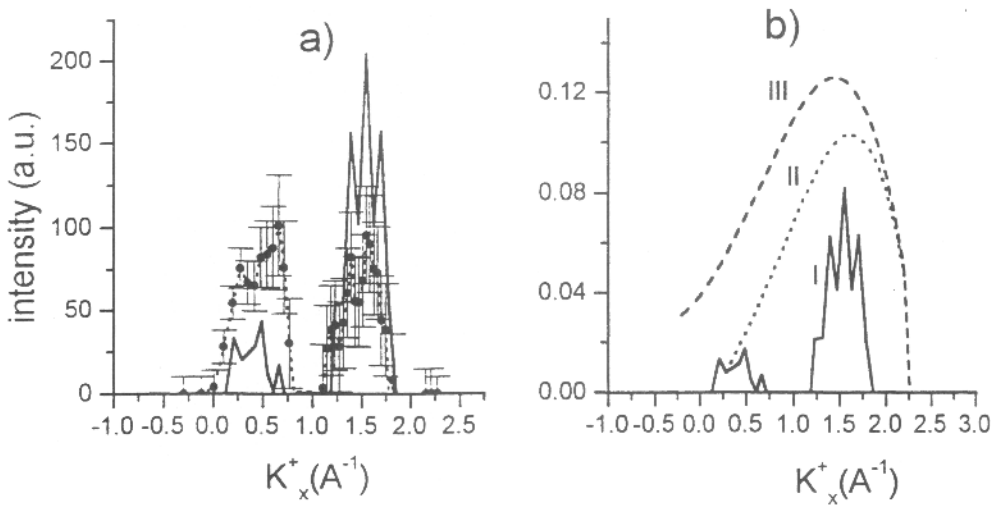

Figure 2: (a) the energy sharing distribution of the difference: [W(001) + 1 ML oxygen] - [clean W(001)]. The total energy of pairs is $24.5 \pm 1\, eV$. The scattering geometry is shown in Fig. (1b). The solid curve is the theoretical results, as deduced from Eq.(8). A uniform energy resolution of $3\, eV$ has been assumed (see text for more calculational details). b) For the same scattering geometry as in (a), the K_x^+-spectrum for pairs emitted from free oxygen atom (dotted curve) and one oxygen atom deposited on tungesten (dashed curve) are shown.

the detectors, $\mathbf{K}_x^+$, that is given by

$$\mathbf{K}_x^+ = 0.363 \left(\sqrt{E_{tot} + \Delta} \cos\alpha_1 - \sqrt{E_{tot} - \Delta} \cos\alpha_2 \right) \tag{11}$$

where α_j, $j = 1, 2$ are the emission angles of the electrons with respect to the surface and $\Delta = E_1 - E_2$.

The K_x^+ distribution of the electron-pair emission intensity is shown in Fig.2. Two pronounced maxima are observed at $K_x^+ = 0.5\, A^{o-1}$ and $K_x^+ = 1.5\, A^{o-1}$. Also depicted in Fig.2 are the theoretical results, as yielded by Eq.(8). The final state is given by Eq.(5), i. e. the electron-electron interaction is taken to all orders in the final state. To calculate (exactly) the integrals (9,10) we employ for the wavefunction φ a single zeta $2p$ state. The cross section is then obtained from Eqs.(1,8) after averaging over initial state magenetic sublevels and summing over the spins' degrees of freedom of the emitted pair. The positions of the maxima are reproduced by the theory, however, the theory predicts different ratio of the magnitude of the peaks. The reason for this shortcoming is comprehensible if we consider the pair emission from a free oxygen atom and from one atom deposited on tungesten. The results for both cases are depicted in Fig.2b. As clear from Fig.2 the cross section for the pair's emission from a free or tungesten-deposited oxygen atom is small around the region of the smaller peak in the spectrum of pair emission from one monolayer. Thus we conclude that the origin of the asymmetric heights of the theoretical peaks in Fig.2a can be traced back

to the behaviour of the atomic ionization cross section, as depicted in Fig.2b. Further effects to be included in theory are the distortion and dispersion of the $2p$ symmetry of the initially bound state and the inclusion of the next order hopping integrals.

5. CONCLUSIONS

In this experimental and theoretical study we investigated the electron-pair emission from adsorbate states of p(2x1) oxygen layer on W(001). The surface sensitivity of the method has been demonstrated by studying the dependence of the emitted electrons' spectra on the amount of coverage. In addition we observed the pair's diffraction from the superlattice. The theoretical calculations including the electron-electron correlation to infinite order reproduce the general shape of the spectrum. However, considerable deviations between theory and experiment are observed.

References

[1] A.M. Bradshow, D. Menzel, and M. Steinkilberg. Japan. J. Appl. Phys. Suppl.2, Pt.2, 841-846. (1974).

[2] N.R. Avery, Surf. Sci., 111, 358 (1981).

[3] Paul E. Luscher. F.M. Propst, J. Vac. Sci. Technol.., 14, No. 1, 400 (1977).

[4] D.R. Mullins and S.H. Overbury, Surf. Sci., 210, 481 (1989).

[5] Shang-Lin Weng, E.W. Plummer, and T. Gustafsson, Phys. Rev. B18, No. 4, 1718 (1978).

[6] I.E. McCarthy and E. Weigold, Rep. Prog. Phys. 54, 789 (1991).

[7] M. Vos, I.E. McCarthy, J. El. Spectr. and Rel. Phenomena, 74, 15 (1995).

[8] M. Vos, I.E. McCarthy, Review of Modern Physics, 67, No.3, 713 (1995).

[9] M. Vos, S.A. Canney, P. Storer, I.E. McCarthy, E. Weigold, Surf. Sci., 327, 387 (1995).

[10] J. Kirschner, O.M. Artamonov, S.N. Samarin, Phys. Rev. Lett., 75, No. 12, 2424 (1995).

[11] S.N. Samarin, O.M. Artamonov, H. Schwabe and J. Kirschner, in the book *Coincidence Studies of Electron and Photon Impact Ionization*, edited by Whelan and Walters, Plenum Press, New York, 271 (1997).

[12] O.M. Artamonov, S.N. Samarin, J. Kirschner, Appl. Phys. A 65, 535 (1997).

[13] S. Samarin, R. Herrmann, H. Schwabe, O. Artamonov, J. El. Spectr. and Rel. Phenomena. *in press*.

[14] J. Berakdar, S. Samarin, R. Herrmann, J. Kirschner, Phys. Rev. Lett, 1998 *in press*